Journal Name

ARTICLE

Bis(imino)pyridines fused with 6- and 7-membered carbocylic rings as *N,N,N*-scaffolds for cobalt ethylene polymerization catalysts

Received 00th January 20xx,
Accepted 00th January 20xx

DOI: 10.1039/x0xx00000x

www.rsc.org/

Zheng Wang,[a,b,c] Yanping Ma,[a] Jingjing Guo,[a] Qingbin Liu,[c,*] Gregory A. Solan,[a,d,*] Tongling Liang,[a] and Wen-Hua Sun[a,b,e,*]

The unsymmetrical diketone, 1,2,3,7,8,9,10-heptahydrocyclohepta[*b*]quinoline-4,6-dione, based on a central pyridine unit fused by both 6- and 7-membered rings, has been synthesized *via* a sequence of reactions including a ruthenium-catalyzed coupling cyclization. Templating this diketone with a mixture of cobalt(II) chloride hexahydrate and the corresponding aniline in acetic acid at reflux afforded five examples of carbocyclic-fused bis(arylimino)pyridine-cobalt(II) chlorides (aryl = 2,6-Me_2Ph **Co1**, 2,6-Et_2Ph **Co2**, 2,6-i-Pr_2Ph **Co3,** 2,4,6-Me_3Ph **Co4**, 4-Me-2,6-Et_2Ph **Co5**) in good yield. All cobalt complexes have been fully characterized including by ^{1}H NMR spectroscopy which reveals broad but assignable paramagnetically shifted peaks. The molecular structures of **Co1**, **Co3** and **Co4** highlight the inequivalency of the two fused rings with the cobalt center adopting a distorted trigonal bipyramidal geometry. Treatment of **Co1** – **Co5** with MAO gave highly active catalysts (up to 5.03 × 10^6 g PE mol^{-1} (Co) h^{-1} at 40 °C, with **Co4** > **Co5** > **Co1** > **Co2** > **Co3**) for ethylene polymerization generating strictly linear vinyl-terminated polymers with low molecular weights (M_w range: 1.53 – 22.77 kg mol^{-1}). By comparison, polymerizations conducted using **Co1** – **Co5**/MMAO were less active and displayed a lower selectivity for unsaturated polymers. Common to both MAO and MMAO, the most sterically hindered precatalyst **Co3** gave the highest molecular weight polymer of the series (up to 22.77 kg mol^{-1}) but exhibited the lowest activity.

Introduction

The capacity of bis(imino)pyridines (**A**, Chart 1) to serve as effective supports for iron and cobalt catalysts for ethylene polymerization has been known since the late 1990s.[1,2] Indeed, this family of homogeneous catalysts has proved not only highly active for ethylene polymerization but also for oligomerization yielding α-olefins with Schulz–Flory distributions.[3] In the intervening years much effort has been directed towards modifying **A** with a view to enhancing the thermo-stability of the catalyst, increasing the activity and broadening the range of olefinic products.[3,4] Elsewhere, alternative *N,N,N*-ligand frames such as 2-imino-1,10-phenanthrolines,[5] 2-benzimidazolyl-6-iminopyridines,[6] *N*-[(pyridin-2-yl)methylene]-8-aminoquinolines,[7] 2,8-bis(imino)-quinolines,[8] have also shown their suitability as supports for the active catalyst. Of particular note, an iminophenanthroline-iron complex has been successfully employed as a catalyst to make α-olefins on in a 500 ton pilot plant operated by Sinopec in China.[3a,3e,5c]

More recently, our group has focused on the tuning of catalyst performance through the introduction of controlled amounts of ring strain to **A**.[3a,3c-e] To realize this goal, tridentate ligand sets have been developed incorporating one[9-11] or two[12-14] cycloalkyl units fused to the central pyridine donor with rings sizes ranging from five to eight (*e.g.*, **B**[12], **C**[13] and **D**[14] in Chart 1). With particular regard to cobalt catalysts, we have observed significant differences in performance between catalysts bearing **B**, **C** and **D**. For example, ($\mathbf{B}_{mesityl}$)Co-type catalysts display reasonable catalytic activity but generate mixtures of oligomers and low molecular weight polymer at low pressure (P_{C2H4} = 1.3 bar),[12] while their larger

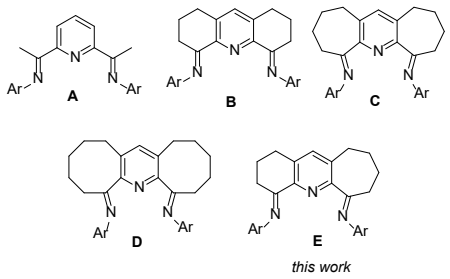

Chart 1. Bis(imino)pyridine **A** and its carbocyclic-fused ring derivatives **B** – **E**.

[a] *Key Laboratory of Engineering Plastics and Beijing National Laboratory for Molecular Science, Institute of Chemistry, Chinese Academy of Sciences, Beijing 100190, China.*
[b] *CAS Research/Education Center for Excellence in Molecular Sciences, University of Chinese Academy of Sciences, Beijing 100049, China.*
[c] *College of Chemistry and Material Science, Hebei Normal University, Shijiazhuang 050024, China.*
[d] *Department of Chemistry, University of Leicester, University Road, Leicester LE1 7RH, UK.*
[e] *State Key Laboratory for Oxo Synthesis and Selective Oxidation, Lanzhou Institute of Chemical Physics, Chinese Academy of Sciences, Lanzhou 730000, China*
**Corresponding Authors: whsun@iccas.ac.cn; liuqingb@sina.com; gas8@leicester.ac.uk (G.A.S.), Tel: +86-10-62557955; Fax: +86-10-62618239.*
Electronic Supplementary Information (ESI) available: Figures, tables, and giving NMR spectra of the new compounds and X-ray crystallographic data in CIF for CCDC 1835457 (**Co1**), 1835458 (**Co3**) and 1835462 (**Co4**) available free of charge from the Cambridge Crystallographic Data Centre. See DOI: 10.1039/x0xx00000x

ring ($\mathbf{C}_{mesityl}$)Co-counterparts, are both more active and selective by forming narrowly dispersed linear polymer ($M_w \approx 10^4$ g mol^{-1}).[13a] On the other hand, their more flexible ($\mathbf{D}_{mesityl}$)Co-comparators containing eight-membered rings, maintain high activity and form higher molecular weight polyethylene ($M_w \approx 10^5$ g mol^{-1}).[14]

Given the marked variation in performance highlighted above, we were interested in exploring what effect a catalyst incorporating two different fused ring sizes would have. In particular, this work is concerned with a novel hybrid class of cobalt catalyst bound by **E** (Chart 1), in which six- and seven-membered rings are fused to the same pyridine. The differing degrees of flexibility imparted by the two different ring systems in **E** make their spatial characteristics quite distinct when compared to their symmetrical counterparts **B**, **C** and **D**. Five examples of **E** have been prepared in which the steric and electronic profile of the N-aryl groups has been systematically varied; full characterization of the resulting complexes and organic precursors is given. Moreover, a comprehensive ethylene polymerization screen is reported in which catalyst optimization is performed using two different aluminoxane co-catalysts. Full details of correlations between precatalyst structure and catalyst performance and polymer structure are detailed and then compared to that observed for catalysts bearing symmetrical **A**, **B**, **C** and **D** (Chart 1).

Results and Discussion

Unlike the diketone precursors to **A** – **D** (Chart 1), the corresponding carbonyl compound, 1,2,3,7,8,9,10-heptahydrocyclohepta[*b*]-quinoline-4,6-dione (**3**), required to make **E** is not available by routine procedures. However, to achieve the synthesis of **3** we devised a three-step route (Scheme 1). Firstly, a ruthenium catalyzed coupling cyclization of (2-aminophenyl)methanol with cycloheptanol gave 6,7,8,9,10-pentahydro-cyclohepta[*b*]quinoline (**1**) in good yield.[15] Subsequently the arene ring in **1** was selectively reduced to 1,2,3,4,6,7,8,9,10-nonahydrocyclohepta[*b*]quinoline (**2**) in high yield by hydrogenation with 10% Pd/C in trifluoroacetic acid.[16] To convert **2** to **3**, **2** was condensed with benzaldehyde and the resulting intermediate oxidized with ozone in dichloromethane at – 60 °C affording **3** on the ten gram scale.[13,14,17] All the new organic compounds, **1** – **3**, have been characterized by FT-IR, ^{1}H/^{13}C NMR spectroscopy (Figures S1 – S6 in SI) and elemental analysis.

In the first instance, we attempted to prepare the free fused bis(imino)pyridines by the condensation reaction of the ketone **3** with the corresponding aniline.[13,14] Unfortunately, the targeted 4,6-bis(arylimino)-1,2,3,7,8,9,10-heptahydro-cyclohepta[*b*]quinolines were not amenable to isolation, an observation that has been noted for some related fused bis(imino)pyridines.[11c,11d,12-14] To circumvent this difficulty, a template methodology was applied to synthesize the cobalt complexes directly using reaction conditions outlined elsewhere.[13,14] Hence, reaction of **3** with a mixture of the corresponding aniline and cobalt dichloride hexahydrate in acetic acid at reflux afforded, on work-up, the 4,6-bis(arylimino)-1,2,3,7,8,9,10-heptahydrocyclohepta[*b*]quinolone-cobalt(II) chlorides (aryl = 2,6-Me_2Ph **Co1**, 2,6-Et_2Ph **Co2**, 2,6-*i*-Pr_2Ph **Co3**, 2,4,6-Me_3Ph **Co4**, 4-Me-2,6-Et_2Ph **Co5**) in good yield (75 – 90%, Scheme 1). All the new cobalt complexes have been characterized

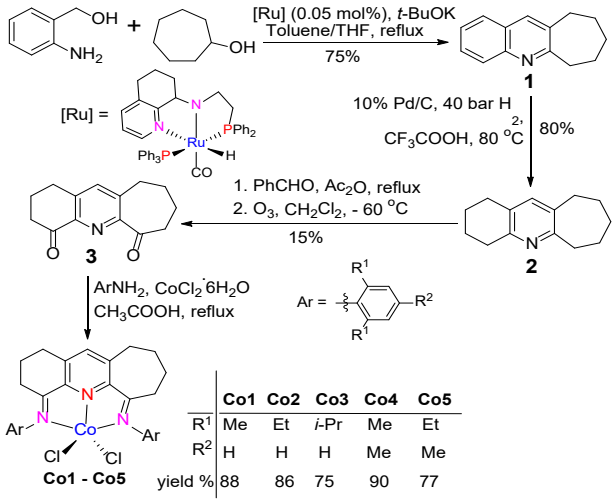

	Co1	Co2	Co3	Co4	Co5
R^1	Me	Et	*i*-Pr	Me	Et
R^2	H	H	H	Me	Me
yield %	88	86	75	90	77

Scheme 1. Synthetic route to **Co1** – **Co5** *via* **1** – **3**

by ^{1}H NMR, FT-IR spectroscopy and elemental analysis, while **Co1**, **Co3** and **Co4** have been the subject of single crystal X-ray diffraction studies.

In the ^{1}H NMR spectra of **Co1** – **Co5**, recorded in $CDCl_3$ at ambient temperature, broad paramagnetically shifted peaks are a feature of all the complexes (Figures S7 – S11). The assignment of the peaks has been made through a comparison with data recorded for related Co(II) (S = 3/2) complexes, relative integration and proximity to the paramagnetic center.[2b,2d,2e,14] Using **Co3** as an example, a downfield peak for the *para*-pyridyl proton at δ 52.32 (***a***) is clearly visible, which is consistent with that reported elsewhere.[2b] While the inequivalent *meta*-aryl protons can be seen more upfield at δ 8.83 (***b*** for Ar_{hep}-H_m) and 36.47 (***c*** for Ar_{hex}-H_m) (Figure 1). Likewise the ketimine methylene protons are inequivalent and appear at δ 8.71 (***d*** for N=C_{hep}-CH_2) and δ 15.53 (***e*** for N=C_{hex}-CH_2) with the *para*-aryl protons at δ -8.24 (***j*** for Ar_{hep}-H_p) and δ -9.11 (***k*** for Ar_{hex}-H_p). In addition and similar to a previous report,[2b] five broad upfield peaks ranging from δ -16.70 to -86.58 can be assigned to the isopropyl protons ***l*** (-16.70, *i*-Pr-Me_{hep}), ***m*** (-17.52, *i*-Pr-Me_{hex}), ***n*** (-21.68, *i*-Pr-Me_{hex}), ***o*** (-79.74, *i*-Pr-CH_{hep}) and ***p*** (-86.58, *i*-Pr-CH_{hex}); the cycloalkyl methylene protons (CH_2) are seen as a series of broad peaks (***f*** - ***i*** and ***q***) between δ 11.26 – 1.20. In the FT-IR spectra of **Co1** – **Co5**, stretching frequencies for the C=N

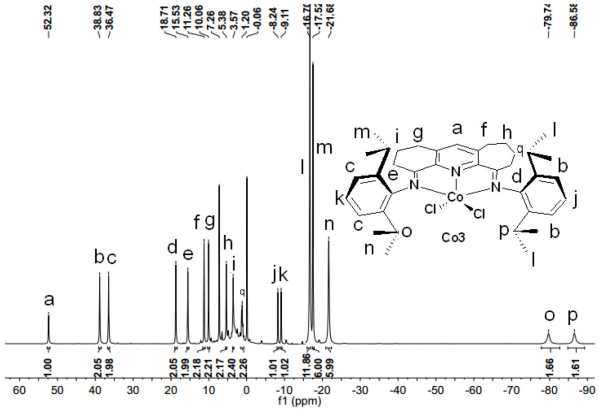

Figure 1. ^{1}H NMR spectrum of **Co3**; recorded in $CDCl_3$ at room temperature.

bonds fall in the range 1613 – 1624 cm^{-1}, characteristic of bound imino-nitrogen atoms; no absorption bands corresponding to a complexed ketonic C=O group[18] nor to free diketone **3** were visible.[13,14]

Crystals of **Co1**, **Co3** and **Co4** suitable for the X-ray determinations were grown by slow diffusion of diethyl ether into a dichloromethane solution of the corresponding complex at ambient temperature. Perspective views of **Co3** and **Co4** are depicted in Figures 2 and 3, while that for **Co1** is presented in the SI (Figure S21); selected bond lengths and angles for all three complexes are collected in Table 1. As a feature apparent to all three structures, the six- and seven-membered rings are disordered across both fused positions. Each molecular structure comprises a single cobalt center surrounded by two chlorides and three nitrogen atoms belonging to the corresponding *N,N,N*-ligand so as to complete a geometry that can be best described as distorted trigonal-bipyramidal. The equatorial belt is filled by the N_{py} atom and the two chloride atoms, while the two N_{imine} atoms occupy the axial positions. The main structural difference between the two complexes arises from the variation of the substituents on the N-aryl groups of the ligand backbone (2,6-dimethylphenyl (**Co1**), 2,6-diisopropylphenyl (**Co3**), mesityl (**Co4**)). In all three structures, the Co-N_{py} bond length is significantly shorter (2.052(4) Å (**Co1**), 2.040(1) Å (**Co3**), 2.040(5) Å (**Co4**)) than the exterior Co-N_{imine} bonds (2.263(3) Å (**Co1**), 2.204(1), 2.202(1) Å (**Co3**), 2.271(4) Å (**Co4**)). Indeed, these Co-N_{py} bond distances are shorter than that observed in cobalt complexes containing **C**[13a] (2.082(3) Å) and **D**[14] (range: 2.0720(18) – 2.0790(2) Å), but close to that found in **A** (2.051(3) Å)[2b] and **B** (2.037(4) Å) (Chart 1).[12] By contrast, the Co–N_{imine} bonds (2.263(3) Å (**Co1**), 2.204(1), 2.202(1) Å (**Co3**), 2.271(4) Å (**Co4**)) are longer than found in complexes of **C**[13a] (2.128(3) and 2.176(3) Å) and **D**[14] (range: 2.1180(18) – 2.1633(18) Å), but similar to those observed with **A**[2b] and **C**[13a] (range: 2.193 – 2.320 Å). The N–Co(1)–N angles within each five-membered chelate ring (75.18(8)° (**Co1**), 75.07(6), 73.97(6)° (**Co3**), 75.30(10)° (**Co4**)) are comparable with that seen in related bis(imino)pyridine-cobalt(II) halide structures,[9,10a,11a,12,13a,14] while the corresponding N–C–C–N torsion angles [3.85° (**Co1**) 7.19°, - 6.34° (**Co3**), 6.59° (**Co4**)] highlight the deviation from co-planarity between the pyridine ring and the

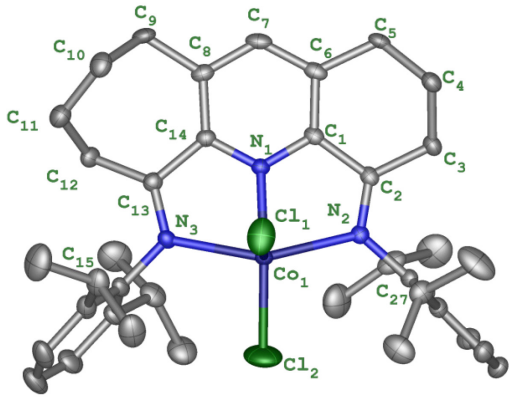

Figure 2. OLEX2 representation of **Co3**; the thermal ellipsoids are shown at 30% probability while the hydrogen atoms have been omitted for clarity.

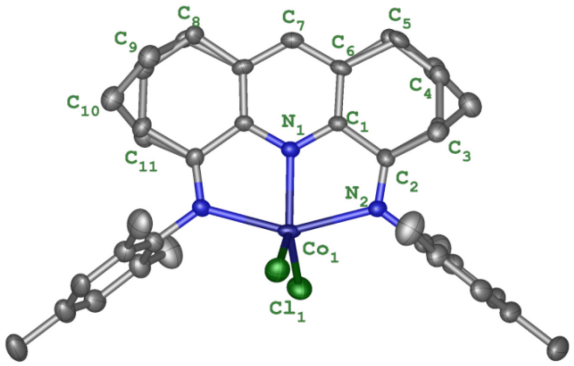

Figure 3. OLEX2 representation of **Co4** showing the positional disorder of the fused rings; the thermal ellipsoids are shown at 30% probability while the hydrogen atoms have been omitted for clarity.

Table 1. Selected bond lengths and angles for **Co1**, **Co3** and **Co4**

Co1		**Co3**		**Co4**	
Bond lengths [Å]					
Co(1)-Cl(1)	2.262(1)	Co(1)-Cl(1)	2.301(3)	Co(1)-Cl(1)	2.253(15)
Co(1)-Cl(1)^{i}	2.262(1)	Co(1)-Cl(2)	2.234(2)	Co(1)-Cl(1)^{i}	2.253(15)
Co(1)-N(2)	2.263(3)	Co(1)-N(2)	2.204(1)	Co(1)-N(2)	2.271(4)
Co(1)-N(2)^{i}	2.263(3)	Co(1)-N(3)	2.202(1)	Co(1)-N(2)^{i}	2.271(4)
Co(1)-N(1)	2.052(4)	Co(1)-N(1)	2.040(1)	Co(1)-N(1)	2.040(5)
Bond angles [°]					
Cl(1)–Co(1)-Cl(1)^{i}	111.67(8)	Cl(1)–Co(1)-Cl(2)	115.67(9)	Cl(1)–Co(1)-Cl(1)^{i}	115.89(9)
N(2)^{1}–Co(1)–Cl(1)	99.20(9)	N(2)–Co(1)–Cl(1)	102.15(10)	N(2)^{1}–Co(1)–Cl(1)	99.57(12)
N(2)–Co(1)–Cl(1)	97.32(9)	N(2)–Co(1)–Cl(2)	99.73(6)	N(2)–Co(1)–Cl(1)	95.92(11)
N(2)–Co(1)–Cl(1)^{i}	99.20(9)	N(3)–Co(1)–Cl(1)	99.73(10)	N(2)–Co(1)–Cl(1)^{i}	99.57(12)
N(2)^{1}–Co(1)–Cl(1)^{i}	97.32(9)	N(3)–Co(1)–Cl(2)	98.49(6)	N(2)^{1}–Co(1)–Cl(1)^{i}	95.91(11)
N(2)^{1}–Co(1)–N(2)	150.4(2)	N(3)–Co(1)–N(2)	141.76(6)	N(2)^{1}–Co(1)–N(2)	150.6(2)
N(1)–Co(1)–Cl(1)	124.17(4)	N(1)–Co(1)–Cl(1)	89.97(8)	N(1)–Co(1)–Cl(1)	122.05(5)
N(1)–Co(1)–Cl(1)^{i}	124.17(4)	N(1)–Co(1)–Cl(2)	154.29(7)	N(1)–Co(1)–Cl(1)^{i}	122.05(5)
N(1)–Co(1)–N(2)	75.18(8)	N(1)–Co(1)–N(2)	75.07(6)	N(1)–Co(1)–N(2)	75.30(10)
N(1)–Co(1)–N(2)^{i}	75.18(8)	N(1)–Co(1)–N(3)	73.97(6)	N(1)–Co(1)–N(2)^{i}	75.30(10)

Atoms labelled 'i' have been generated by symmetry

neighboring imine vectors. Notably, these deviations are comparable to that seen in **C** (6.6(4)°, -6.0(4)°),[13a] but smaller than that seen in the eight-membered ring analogue **D** (8.90°, -15.06°).[14] As expected the saturated sections of the six- and seven-membered rings adopt puckered arrangements with relatively more flexibility a feature of the larger ring. Similar to the majority of structurally characterized bis(imino)pyridine-cobalt complexes, the N-aryl rings in each structure are close to perpendicular with respect to their neighboring imine vectors. There are no intermolecular contacts of note in either structure.

Catalytic evaluation

Based on previous findings for structurally related cobalt(II) chloride complexes (*e.g.*, **A** – **D** in Chart 1),[2b,9b,10a,11,12a,b,13a,14] the highest catalytic activity for ethylene polymerization tends to be observed on activation with either methylaluminoxane (MAO) or modified MAO (MMAO).[1,2,10-14] Hence, the current investigation focuses on these two aluminoxane co-catalysts with **Co4** (2,4,6-trimethylphenyl) selected as the test precatalyst. All the resultant polymers have been characterized by gel permeation chromatography (GPC) and differential scanning calorimetry (DSC), while the microstructural properties of selected samples were examined using high temperature ^{1}H NMR and ^{13}C NMR spectroscopy. In all cases gas chromatography was used to detect the presence of any oligomeric products.

Ethylene polymerization with the Co1 – Co5/MAO

With the intent to establish the optimum polymerization conditions for **Co4** with MAO as co-catalyst, different Al/Co molar ratios, reaction temperatures and run times were all systematically explored; the results of the polymerization runs are collected in Table 2. With the ethylene pressure set at 10 atm and the temperature at 30 °C, the Al/Co ratio was varied from 1000 to 2500 (entries 1 – 6, Table 2) over a thirty-minute run time. A peak in catalytic activity of 3.95×10^6 g PE mol^{-1}(Co) h^{-1} was observed at a ratio of 1500 (entry 3, Table 2) affording a polymeric product; no trace of short chain oligomers could be detected. The polymers are of low molecular weight falling in the range 1.63 to 2.03 kg mol^{-1}, which are characteristic of polyethylene waxes. As shown by their GPC curves in Figure 4, the molecular weights of the polymers gradually decrease (from 2.03 to 1.63 kg mol^{-1}) on increasing the Al/Co molar ratio.[2b,9b,11a,11b,13a,14]

Subsequently, the influence of reaction temperature was investigated with the Al/Co molar ratio fixed at 1500. On elevating the temperature from 20 to 60 °C (entries 3 and 7 – 10, Table 2), the highest activity (5.03×10^6 g PE mol^{-1} (Co) h^{-1}) was observed at 40 °C (entry 8, Table 2). Moreover, the molecular weights of the polyethylenes gradually decreased (from 1.76 to 1.35 kg mol^{-1}, Figure 5) with increasing temperature which can be accredited to a higher rate of chain transfer relative to chain propagation at elevated temperature. Once again all the polymers were obtained as waxes with molecular weights falling typically in the thousands, while the molecular weight distributions were narrow (*Đ* range: 1.5 – 1.7); these narrow values of *Đ* could be attributed to single-site behavior[9b,11a,11b,13a] or could be explained by efficient alkyl chain shuttling between aluminum and the catalyst.[19]

Table 2. Polymerization screening using **Co1** - **Co5**/MAO

Run	Precat.	Al/Co	T (°C)	t (min)	Yield (g)	Activity[b]	M_w[c]	*Đ*[c]	T_m (°C)[d]
1	**Co4**	1000	30	30	2.20	1.47	2.03	1.6	121.4
2	**Co4**	1250	30	30	4.75	3.17	1.74	1.6	121.5
3	**Co4**	1500	30	30	5.92	3.95	1.63	1.7	121.2
4	**Co4**	1750	30	30	4.95	3.30	1.68	1.6	121.6
5	**Co4**	2000	30	30	4.56	3.04	1.65	1.6	121.7
6	**Co4**	2500	30	30	3.95	2.63	1.68	1.6	121.3
7	**Co4**	1500	20	30	3.67	2.45	1.76	1.6	121.9
8	**Co4**	1500	40	30	7.55	5.03	1.53	1.6	121.8
9	**Co4**	1500	50	30	6.40	4.27	1.40	1.5	121.7
10	**Co4**	1500	60	30	3.36	2.24	1.35	1.5	121.6
11	**Co4**	1500	40	5	2.38	9.52	1.49	1.6	121.5
12	**Co4**	1500	40	15	4.80	6.40	1.56	1.6	121.2
13	**Co4**	1500	40	45	7.65	3.40	1.61	1.5	121.2
14	**Co4**	1500	40	60	7.85	2.61	1.71	1.6	121.4
15[e]	**Co4**	1500	40	30	2.75	1.83	1.71	1.5	121.1
16[f]	**Co4**	1500	40	30	0.50	0.33	1.07	1.3	119.0
17	**Co1**	1500	40	30	4.75	3.17	1.64	1.5	121.8
18	**Co2**	1500	40	30	3.90	2.60	3.67	1.9	121.7
19	**Co3**	1500	40	30	3.16	2.11	22.77	1.9	131.4
20	**Co5**	1500	40	30	4.80	3.20	3.79	1.9	126.3

[a] Conditions: 3.0 µmol of cobalt precatalyst; 100 mL toluene, 10 atm C_2H_4. [b] Values in units of 10^6 g(PE) mol^{-1} (Co) h^{-1}. [c] Determined by GPC, M_w in kg mol^{-1}. [d] Determined by DSC. [e] 5 atm C_2H_4. [f] 1 atm C_2H_4.

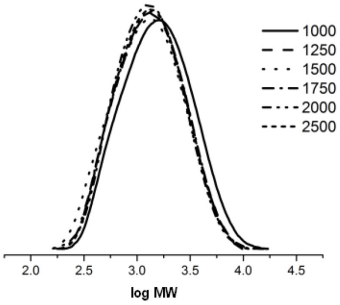

Figure 4. GPC curves of the polyethylenes obtained using **Co4**/MAO with various Al/Co ratios; T = 30 °C and P_{C2H4} = 10 atm.

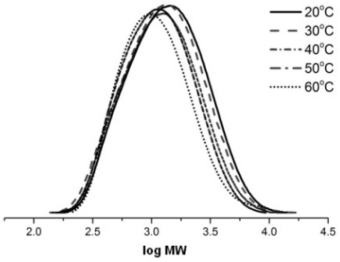

Figure 5. GPC curves of the polyethylenes obtained using **Co4**/MAO at different reaction temperatures; P_{C2H4} = 10 atm, Al/Co ratio = 1500 and run time = 30 min.

In order to investigate the lifetime of the active species and the effect of the reaction time on the polymerization, the tests were conducted over different reaction times from 5 to 60 minutes (entries 8 and 11 – 14, Table 2). The topmost activity (9.52 × 10^6 g PE mol^{-1} (Co) h^{-1}) was achieved after 5 minutes which then gradually decreased (2.61 × 10^6 g PE mol^{-1} (Co) h^{-1}) after 60 minutes, which can be attributed to the active species being formed quickly after the addition of MAO and then becoming gradually deactivated over extended reaction times.[13a,14,20] In addition, the polymers displayed progressively increasing molecular weights over time (from 1.49 to 1.71 kg mol^{-1}), which suggests that despite catalyst deactivation sufficient species remained present to promote chain growth.[13a,14] With the ethylene pressure reduced to 5 atm (entry 15, Table 2), the activity was less than half of that at 10 atm (entry 8, Table 2) and almost six times less at 1 atm (entry 16, Table 2).

Using the optimized conditions established for **Co4**/MAO (*i.e.*, Al/Co ratio of 1500, 40 °C and 30 minutes), the remaining cobalt complexes, **Co1** - **Co3** and **Co5**, were additionally screened as precatalysts for ethylene polymerization. Inspection of the data reveals that all the MAO-activated systems showed high activities (entries 17 – 20, Table 2), with their relative values decreasing in the order: **Co4** (2,4,6-trimethyl) > **Co5** (4-methyl-2,6-diethyl) > **Co1** (2,6-dimethyl) > **Co2** (2,6-diethyl) > **Co3** (2,6-diisopropyl) (entries 8 and 18 - 20, Table 2). This trend is similar to that observed with cobalt precatalysts bearing **C**-type ligands,[13a] in which both steric and electronic properties are influential.[2b,13a,14,21] For example, the activity with the most hindered system **Co3** (2,6-diisopropyl) shows the lowest activity (2.11 × 10^6 g PE mol^{-1} (Co) h^{-1}) which implies the bulky substituents impede the coordination and insertion of ethylene. In terms of electronic effects, the presence of the

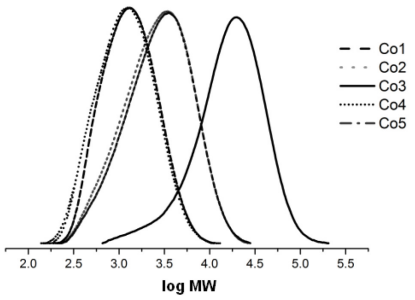

Figure 6. GPC curves of the polyethylenes obtained using **Co1** - **Co5**/MAO; P_{C2H4} = 10 atm, Al/Co ratio = 1500, T = 40 °C and run time = 30 min.

donating methyl groups at the *para*-position results in the best catalytic activity; the enhanced solubility of these complexes as a result of the additional aliphatic (*para*-methyl) group may also be a contributing factor.[12a,12b,13a,14] With regard to molecular weight, the polyethylene obtained with **Co3** exhibited by far the highest molecular weight (22.77 kg mol^{-1}, entry 19, Table 2) of the series, which also highlights the role played by the bulky substituent in inhibiting chain transfer during the polymerization (Figure 6).[2b,9a,9b,13a,14] In any case, polyethylene waxes displaying narrow polydispersity (*Đ* range: 1.6 – 1.9) are a feature of all the materials.

For the purposes of comparison, the activity and molecular weight data for the polymer samples generated using ($\mathbf{A}_{mesityl}$)$CoCl_2$/MAO, ($\mathbf{B}_{mesityl}$)$CoCl_2$/MAO, ($\mathbf{C}_{mesityl}$)$CoCl_2$/MAO, ($\mathbf{D}_{mesityl}$)$CoCl_2$/MAO (Chart 1) and **Co4**($\mathbf{E}_{mesityl}$)/MAO at 40 °C are displayed in Figure 7 (see SI, Tables S2 - S6). To maintain consistent conditions for all five systems, the polymerization data for ($\mathbf{B}_{mesityl}$)$CoCl_2$/MAO had to be re-determined at 10 atm C_2H_4 (see SI, Table S3) as the original report used lower pressure.[12] All the MAO-activated systems showed high activities (up to 10^6 g(PE) mol^{-1} (Co) h^{-1}), with their relative values decreasing in the order: **Co4** (**E**) > ($\mathbf{A}_{mesityl}$)$CoCl_2$ > ($\mathbf{C}_{mesityl}$)$CoCl_2$ > ($\mathbf{B}_{mesityl}$)$CoCl_2$ > ($\mathbf{D}_{mesityl}$)$CoCl_2$. They also formed a wide range of molecular weights from polyethylene waxes to high molecular weight polyethylene, with their relative values, as a function of the precatalyst, decreasing in the order: ($\mathbf{D}_{mesityl}$)$CoCl_2$ > ($\mathbf{B}_{mesityl}$)$CoCl_2$ > ($\mathbf{C}_{mesityl}$)$CoCl_2$ > ($\mathbf{A}_{mesityl}$)$CoCl_2$ > **Co4** (**E**). These trends may be ascribed to a combination of differences in ring flexibility/tension, chelation properties and steric effects of

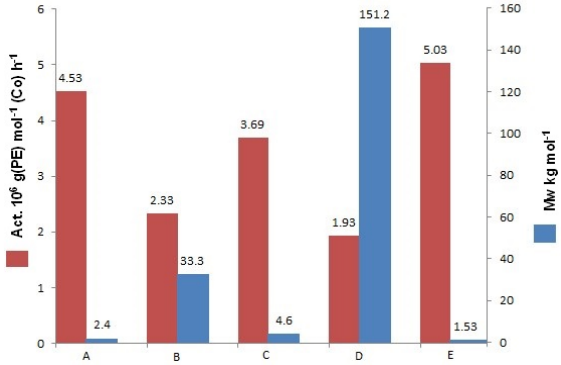

Figure 7. Comparative catalytic performance of **Co4** with cobalt-containing **A**,[2b] **B**[12] **C**[13a] and **D**[14] (Chart 1); all runs conducted using MAO, P_{C2H4} = 10 atm and at 40 °C.

these cycloalkyl-fused bis(arylimino)pyridines. With regard to **Co4** (**E**), the mixed fused rings confer inequivalent levels of steric hindrance as well as different degrees of ring flexibility with the result that this catalyst is the most active but forms the lowest molecular weight polymer. By contrast, ($\mathbf{D}_{mesityl}$)$CoCl_2$, containing the more bulky and most flexible eight-membered rings, was the least active but formed the highest molecular weight polymer. Evidently, the constraints of the various fused ligands impact on when the chain transfer occurs, with **Co4** (**E**) having a predilection towards more facile chain transfer. With regard to polydispersity of the polymers, the current system (*Đ* = 1.5) exhibited the narrowest distribution while the more rigid ($\mathbf{B}_{mesityl}$)$CoCl_2$/MAO was broader (*Đ* = 2.9) and the most flexible system ($\mathbf{D}_{mesityl}$)$CoCl_2$/MAO the broadest (*Đ* = 4.4). Collectively, these data not only highlight the importance of the fused ring size but also the effect of mixed rings on influencing catalytic performance, molecular weight and dispersity.[1,11,13a,14]

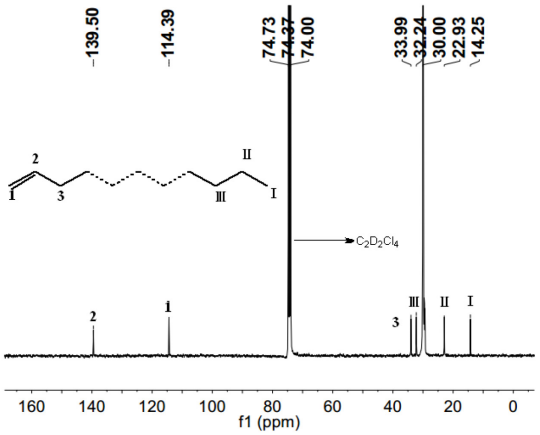

Figure 8. ^{13}C NMR spectrum of the polyethylene obtained using **Co4**/MAO at 40 °C (entry 8, Table 2); recorded in 1,1,2,2-tetrachloroethane-d_2 (δ C 74.2) at 100 °C.

In terms of the polymers generated using **Co1** – **Co5**, the melting temperatures were all around 120 °C (Table 2), which suggests high linearity. To verify this conclusion the microstructure of the polyethylene obtained by **Co4** at 40 °C (entry 8, Table 2) was investigated by high temperature ^1H NMR and ^{13}C NMR spectroscopy (recorded in 1,1,2,2-tetrachloroethane-d_2 at 100 °C). Examination of the ^{13}C NMR spectrum reveals, as the most intense peak, a signal at δ 30.0 corresponding to the –(CH_2)– repeat unit found in a highly linear polyethylene (Figure 8).[2b,12b,13b,20] In addition, peaks at δ 114.4 (C_1) and 139.5 (C_2) provide evidence for a vinyl end-group (–CH=CH_2), with the more upfield peaks at δ 33.2 (C_{III}), 22.9 (C_{II}) and 14.3 (C_I) in agreement with a saturated propyl end-group. The ^1H NMR spectrum reveals downfield multiplets at δ 5.85 (H_1) and δ 5.03 (H_2/$H_{2'}$) corresponding to the vinylic protons (–CH=CH_2) as well as a more upfield signal to the methyl chain-end (H_I) (Figure 10). The relative integration of H_1:H_2/H_2':H_I reveals a 1:2:3 ratio which further supports the linearity of the polymer chain and indicates that chain termination occurs exclusively *via* β-hydride elimination.[2b,4a,12b,13b,20] It is noteworthy that such vinyl-terminated low molecular weight polymers are in demand for the production of long-chain branched copolymers, functional polymers as well as coating materials.

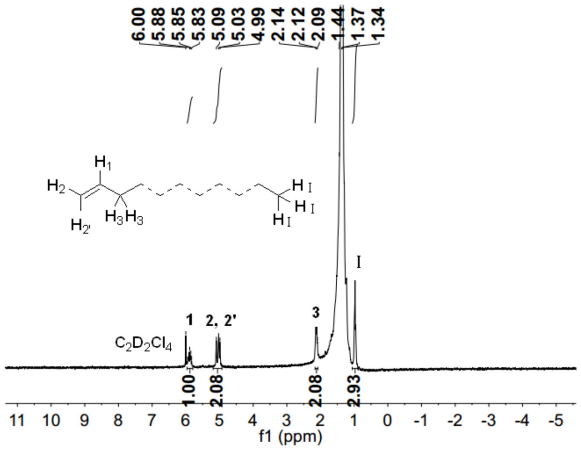

Figure 9. ^1H NMR spectrum of the polyethylene obtained using **Co4**/MAO at 40 °C (entry 8, Table 2); recorded in 1,1,2,2-tetrachloroethane-d_2 at 100 °C.

Ethylene polymerization using Co1 – Co5/MMAO

As with the MAO-promoted polymerizations, **Co4** was once more chosen to optimize the runs using MMAO as the co-catalyst; the results of all the tests are gathered in Table 3. Firstly, on increasing the molar ratio of Al/Co from 1000 to 2500 (entries 1 - 6, Table 3), with the temperature kept at 30 °C and the pressure at 10 atm, a maximum in activity was achieved of 2.37 × 10^6 g PE mol^{-1}(Co) h^{-1} with the ratio at 2000 which compares to 1500 with MAO. As with MAO, the polyethylenes displayed low molecular weights (1.53 - 1.84 kg mol^{-1}) and narrow polydispersities (*Đ* ≈ 1.6) consistent with single-site characteristics for the active species (Figure S18).[13a,19] With the Al/Co molar ratio retained at 2000 and the run time at 30 minutes, the influence of reaction temperature for **Co4**/MMAO was investigated over the 20 – 60 °C range (entries 4 and 7 – 10, Table 3). The highest activity of 2.83 × 10^6 g PE mol^{-1}(Co) h^{-1} was again observed at 40 °C (entry 8, Table 3) which compares with 5.03 × 10^6 g PE mol^{-1} (Co) h^{-1} for **Co4**/MAO. The GPC curves of the polyethylenes obtained at different temperatures show that the polymers with higher molecular weights (up to 1.63 kg mol^{-1} at 20 °C) were obtained at lower reaction temperature without any significant variations in dispersity (Figure S19).

Secondly, in order to explore the lifetime of **Co4**/MMAO, the runs were performed over 5, 15, 30, 45 and 60 minutes with the temperature maintained at 40 °C and the Al/Co ratio at 2000 (entries 8 and 11 – 14, Table 3). The maximum activity of 6.40 × 10^6 g PE mol^{-1} (Co) h^{-1} was observed after 5 minutes (*c.f.* 9.52 × 10^6 g PE mol^{-1} (Co) h^{-1} for **Co4**/MAO), while on prolonging the reaction time the activity gradually decreased.[9,11b,13a,14,20,21] This finding indicates that the active species was quickly formed without any significant induction period and gradually deactivated over time.[13a,14,21] The molecular weights of the polyethylenes increased (from 1.52 to 3.17 kg mol^{-1}) with increasing reaction time as did the dispersities reaching a maximum of 1.9 after 60 minutes (Figure S20).

Thirdly, the remaining four precatalysts (**Co1** – **Co3** and **Co5**) were studied under the optimum conditions (Al/Co ratio of 2000 (MMAO), 40 °C and 30 minutes) and compared with **Co4**/MMAO Collectively, all five cobalt precatalysts showed high activities for ethylene polymerization (entries 8 and 17 – 20, Table 3), though

Table 3. Polymerization screening using **Co1** - **Co5**/MMAO

Run	Precat.	Al/Co	T (°C)	t (min)	Yield (g)	Activity[b]	M_w[c]	$Đ$[c]	T_m[d] (°C)
1	**Co4**	1000	30	30	2.21	1.47	1.84	1.7	122.1
2	**Co4**	1500	30	30	2.50	1.67	1.70	1.6	121.3
3	**Co4**	1750	30	30	3.18	2.12	1.64	1.6	121.0
4	**Co4**	2000	30	30	3.56	2.37	1.53	1.6	121.1
5	**Co4**	2250	30	30	2.32	1.55	1.66	1.6	121.5
6	**Co4**	2500	30	30	1.56	1.04	1.62	1.6	121.8
7	**Co4**	2000	20	30	3.07	2.05	1.63	1.6	121.2
8	**Co4**	2000	40	30	4.25	2.83	1.58	1.6	121.1
9	**Co4**	2000	50	30	3.13	2.09	1.32	1.6	120.9
10	**Co4**	2000	60	30	2.04	1.36	1.25	1.4	120.2
11	**Co4**	2000	40	5	1.60	6.40	1.52	1.5	121.2
12	**Co4**	2000	40	15	2.86	3.81	1.54	1.6	121.5
13	**Co4**	2000	40	45	5.45	2.42	2.24	1.8	121.6
14	**Co4**	2000	40	60	5.85	1.95	3.17	1.9	121.7
15[e]	**Co4**	2000	40	30	1.69	1.12	2.65	1.9	121.2
16[f]	**Co4**	2000	40	30	0.10	0.06	1.24	1.3	121.3
17	**Co1**	2000	40	30	4.96	3.31	1.40	1.6	121.8
18	**Co2**	2000	40	30	4.02	2.68	1.53	1.6	121.3
19	**Co3**	2000	40	30	3.46	2.31	19.38	2.1	131.7
20	**Co5**	2000	40	30	3.75	2.50	3.35	1.9	124.7

[a] Conditions: 3.0 µmol of cobalt precatalyst; 100 mL toluene, 10 atm C_2H_4. [b] Values in units of 10^6 g(PE) mol^{-1} (Co) h^{-1}. [c] Determined by GPC, M_w in kg mol^{-1}. [d] Determined by DSC. [e] 5 atm C_2H_4. [f] 1 atm C_2H_4.

generally lower than that seen with MAO. Moreover, some variation in the order of activities was apparent with *para*-methyl-containing precatalysts no longer showing the higher activities: **Co1** (2,6-dimethyl) > **Co4** (2,4,6-trimethyl) > **Co2** (2,6-diethyl) > **Co5** (2,6-diethyl-4-methyl) > **Co3** (2,6-diisopropyl). Nevertheless, steric factors once again govern the order of activity with increasing hindrance leading to lower activity.[2b,12-14,21] In agreement with the MAO-activated systems, precatalyst **Co3** (2,6-diisopropyl) produced polyethylene with much higher molecular weight (19.38 kg mol^{-1}, entry 19, Table 3) when compared to the polymers generated using **Co1**, **Co2**, **Co4** or **Co5** (entries 8, 17, 18, and 20, Table 3).

To probe and compare the microstructural properties of the polyethylene obtained using **Co4**/MMAO with that for **Co4**/MAO (*vide supra*), a sample prepared at 40 °C (entry 8, Table 3) was the subject of a high temperature $^{13}C/^{1}H$ NMR spectroscopic study (in deuterated 1,1,2,2-tetrachloroethane-d_2 at 100 °C). A singlet peak of high intensity around δ 29.36 in the ^{13}C NMR spectrum (see SI, Figure S14) confirms the high linearity of the polyethylene obtained.[9-11,13,14,22] This finding is further evidenced by its high melting temperature (T_m = 121.1 °C, entry 8, Table 3). Also apparent in the ^{13}C NMR spectrum are lower intensity peaks at δ 32.2, 22.9 and 14.3 corresponding to a *n*-propyl end-group.[4a,4c,18] However, closer inspection of the downfield region shows only weak peaks at δ 113.7 and 138.8 for the unsaturated chain ends (–CH=CH_2). This finding is supported by the appearance of weak downfield multiplets at δ 5.90 and δ 5.05 for the vinylic protons in the ^{1}H NMR spectrum (see SI, Figure S15).[11,13] These observations would suggest that, dissimilar to that seen with MAO at the same temperature, chain termination via β-H elimination is no longer the sole chain transfer pathway operative, with chain transfer to aluminum now competitive. A plausible explanation for this difference in behavior may derive from the higher molar equivalents of MMAO employed in the polymerization run (Al:Co = 2000) as compared to MAO (Al:Co = 1500) and hence the larger amounts of $AlMe_3$ present. This increased concentration would then lead to an increase in the rate of chain transfer and in turn a reduction in chain propagation.[14,23]

To further examine the microstructural properties of the polymers obtained using MMAO as co-catalyst, we also recorded the ^{1}H NMR spectra of the polyethylenes obtained at 30 °C using 1000 (entry 1, Table 3), 1500 (entry 3, Table 3) and 2000 (entry 5, Table 3) equivalents of co-catalyst (with **Co4** as precatalyst) (see SI, Figure S14 – S17). All three spectra are similar revealing, in addition to a high intensity singlet for the –$(CH_2)_n$– repeat unit, lower intensity signals at *ca.* δ 1.00 for the methyl chain-end (H_I) and at *ca.* 5.90 (H_1) and *ca.* δ 5.05 ($H_2/H_{2'}$) for the vinylic protons.[4a,11,13b] The relative integrations for H_1:$H_2/H_{2'}$:H_I shows a ratio of 1:2:4 for 1000 equivalents (see SI, Figure S14), 1:2:5 for 1500 equivalents (see SI, Figure S15) and 1:2:8 for 2000 equivalents (see SI, Figure S16). The results show that increasing the ratio of Al/Co inhibits β-H elimination, while chain transfer to aluminum becomes the dominant pathway for chain termination.[2b,4a,4c]

Conclusions

Using a series of non-routine synthetic procedures, five examples of paramagnetic cobalt(II) chloride complexes (**Co1** – **Co5**), bound by a hybrid bis(imino)pyridine fused with both six and seven-membered rings, have been successfully synthesized and fully characterized. Comparison of the structural properties of these complexes with cobalt comparators containing the symmetrically fused bis(imino)pyridines, **B** (6/6), **C** (7/7) and **D** (8/8) highlights the differences in strain, ring flexibility, steric and chelation properties. Upon activation with MAO or MMAO, **Co1** – **Co5** displayed high

activities (5.03×10^6 g PE mol^{-1} (Co) h^{-1} at 40 °C) for ethylene polymerization forming strictly linear polyethylene waxes with narrow molecular weight distributions. Notably, the polymer formed using MAO as activator displayed a high selectivity for vinyl end-groups (–CH=CH_2), while with MMAO the formation of some fully saturated polyethylenes was competitive. As a general feature, precatalysts bearing relatively small *ortho*-substituents exhibited higher activities compared to those possessing more sterically demanding groups and produced polyethylenes of lower molecular weight. Moreover, these hybrid 6-/7-membered ring catalysts exhibit distinct performances in ethylene polymerization when compared with catalysts derived from **B** (6/6), **C** (7/7) and **D** (8/8), which have been attributed to the variations in the ligand backbone as highlighted above.

Experimental Section

General Considerations.

All manipulations involving air- and moisture-sensitive compounds were carried out under nitrogen atmosphere by using standard Schlenk techniques. Toluene was heated to reflux over sodium and distilled under nitrogen prior to use. MAO [1.46 M solution in toluene, Al concentration as $AlMe_3$ of 0.005 M] and MMAO [1.93 M in *n*-heptane, Al concentration as $AlMe_3$ of 0.005 M and Al concentration as Al(*i*-Bu)$_3$ of 0.004 M] were purchased from Akzo Nobel Corp. High-purity ethylene was purchased from Beijing Yansan Petrochemical Co. and used as received. Other reagents were purchased from Aldrich, Acros or local suppliers. NMR spectra were recorded with a Bruker Avance-III 500 MHz instrument at ambient temperature by using TMS as internal standard. IR spectra were recorded with a PerkinElmer System 2000 FTIR spectrometer. Elemental analysis was carried out with a Flash EA 1112 microanalyzer. Molecular weights and molecular weight distributions of the polymers were determined with an Agilent PLGPC 220 GPC system at 150 °C with 1,2,4-trichlorobenzene as solvent. The melting temperatures of the polyethylenes were measured from the fourth scanning run on a PerkinElmer TA-Q2000 differential scanning calorimeter under a nitrogen atmosphere. A sample of about 5.0 mg was heated to 160 °C at a rate of 20 °C min^{-1}, kept for 2 min at 160 °C to remove the thermal history, and then cooled to –40 °C at a rate of 20 °C min^{-1}. ^{13}C NMR spectra of the polyethylenes were recorded with a Bruker DMX 300 MHz instrument at 100 °C in 1,1,2,2-tetrachloroethane-d_2 with TMS as internal standard. Column chromatography was performed using silica gel (200–300 mesh). The ruthenium catalyst, [*fac*-PNN]RuH(PPh_3)(CO)(PNN = 8-(2-diphenylphosphinoethyl)amidotrihydroquinoline), was prepared using a literature procedure.[15a] The syntheses of **1**, **2** and **3** along with **Co1** - **Co5** are given in the SI.

Polymerization studies

Ethylene polymerization at P_{C2H4} = 5 or 10 atm

The autoclave was evacuated and backfilled with ethylene three times. When the required temperature was reached, the precatalyst (3 μmol) was dissolved in toluene (30 mL) in a Schlenk tube and injected into the autoclave containing ethylene (~ 1 atm) followed by the addition of more toluene (30 mL). The required amount of co-catalyst (MAO and MMAO) and additional toluene were added successively by syringe taking the total volume of solvent to 100 mL. The autoclave was immediately pressurized with 5 or 10 atm pressure of ethylene and the stirring commenced. After the required reaction time, the reactor was cooled with a water bath and the excess ethylene vented. Following quenching of the reaction with 10% hydrochloric acid in ethanol, the polymer was collected and washed with ethanol and dried under reduced pressure at 50 °C and weighed.

Ethylene polymerization at P_{C2H4} = 1 atm

The polymerization at 1 atm ethylene pressure was carried out in a Schlenk tube. Under an ethylene atmosphere (*ca.* 1 atm), **Co4** (3.0 μmol) was added followed by toluene (30 mL) and then the required amount of co-catalyst (MAO, MMAO) introduced by syringe. The solution was then stirred at 40 °C under an ethylene atmosphere (1 atm). After 30 min, the solution was quenched with 10% hydrochloric acid in ethanol. The polymer was washed with ethanol, dried under reduced pressure at 40 °C and then weighed.

X-ray structure determinations

Single-crystal X-ray diffraction studies of **Co1**, **Co3** and **Co4** were conducted on a Rigaku Sealed Tube CCD (Saturn 724+) diffractometer with graphite-monochromated Mo-Kα radiation (λ = 0.71073 Å) at 173(2) K and the cell parameters obtained by global refinement of the positions of all collected reflections. The intensities were corrected for Lorentz and polarization effects and empirical absorption. The structures were solved by direct methods and refined by full-matrix least-squares on F^2. Non-hydrogen atoms were refined anisotropically and all hydrogen atoms placed in calculated positions. Structure solution and refinement were performed by using SHELXT (Sheldrick, 2015).[24] The disorder displayed by the carbon atoms of the fused rings was also processed by the SHELXL software (Sheldrick, 2015).[24b] Crystal data and processing parameters for **Co1**, **Co3** and **Co4** are summarized in the supporting information (Table S1).

Conflicts of interest

There are no conflicts to declare.

Acknowledgements

This work was supported by the National Natural Science Foundation of China (Nos. 21871275 and 51861145303) and UCAS Joint PhD Training Program (UCAS[2017]16). G.A.S. thanks the Chinese Academy of Sciences for a President's International Fellowship for Visiting Scientists.

Notes and references

1. (a) B. L. Small, M. Brookhart, and A. M. A. Bennett, *J. Am. Chem. Soc*., 1998, **120**, 4049–4050; (b) B. L. Small, M. Brookhart, *J. Am. Chem. Soc*., 1998, **120**, 1207143−7144; (c) B. L. Small, M. Brookhart, *Macromolecules*, 1999, **32**, 2120-2130.
2. (a) G. J. P. Britovsek, V. C. Gibson, B. S. Kimberley, P. J. Maddox, S.

J. McTavish, G. A. Solan, A. J. P. White and D. J. Williams, *Chem. Commun*., 1998, 849–850; (b) G. J. P. Britovsek, M. Bruce, V. C. Gibson, B. S. Kimberley, P. J. Maddox, S. Mastroianni, S. J. McTavish, C. Redshaw, G. A. Solan, S. Stromberg, A. J. P. White and D. J. Williams, *J. Am. Chem. Soc*., 1999, **121**, 8728–8740; (c) G. J. P. Britovsek, S. Mastroianni, G. A. Solan, S. P. D. Baugh, C. Redshaw, V. C. Gibson, A. J. P. White, D. J. Williams, M. R. Elsegood. J. Chem. Eur. J. 2000, **6**, 2221–2231; (d) G. J. P. Britovsek, V. C. Gibson, B. S. Kimberley, S. Mastroianni, C. Redshaw, G. A. Solan, A. J. P. White, D. J. Williams, *J. Chem. Soc., Dalton Trans*., 2001, 1639–1644; (e) G. J. P. Britovsek, V. C. Gibson, S. K. Spitzmesser, K. P. Tellmann, A. J. P. White, D. J. Williams, *J. Chem. Soc*., *Dalton Trans*., 2002, 1159–1171.

3. For reviews see: (a) Z. Wang, G. A. Solan, W. Zhang, and W.-H. Sun, *Coord. Chem. Rev*., 2018, **363**, 92–108; (b) B. L. Small, *Acc. Chem. Res*., 2015, **48**, 2599–2611; (c) B. Burcher, P.-A. R. Breuil, L. Magna, and H. Olivier-Bourbigou, *Top Organomet Chem.*, 2015, **50**, 217–258; (d) Z. Flisak, W.-H. Sun, *ACS Catal*., 2015, **5**, 4713–4724; (e) J. Ma, C. Feng, S. Wang, K.-Q. Zhao, W. -H. Sun, C. Redshaw, G. A. Solan, *Inorg. Chem. Front*., 2014, **1**, 14–34; (f) W. Zhang, W. -H. Sun and C. Redshaw, *Dalton Trans*., 2013, **42**, 8988–8997; (f) V. C. Gibson and G. A. Solan, in Catalysis without Precious Metals (Ed. R. M. Bullock), Wiley-VCH, Weinheim, 2010, 111–141; (h) V. C. Gibson and G. A. Solan, *Top. Organomet. Chem*., 2009, **26**, 107–158; (i) V. C. Gibson, C. Redshaw and G. A. Solan, *Chem. Rev*., 2007, **107**, 1745–1776; (j) C. Bianchini, G. Giambastiani, I. G. Rios, G. Mantovani, A. Meli and A. M. Segarra, *Coord. Chem. Rev*., 2006, **250**, 1391–1418; (k) L. Li, P. T. Gomes, *Springer*, 2010, **36**, 77–197.
4. (a) Q. Mahmood, J. Guo, W. Zhang, Y. Ma, T. Liang, and W.-H. Sun, *Organometallics*, 2018, **37**, 957–970; (b) Q. Mahmood, E. Yue, J. Guo, W. Zhang, Y. Ma, X. Hao and W.-H. Sun, *Polymer*, 2018, **159**, 124–137; (c) N. V. Semikolenova, W.-H. Sun, I. E. Soshnikov, M. A. Matsko, O. V. Kolesova, V. A. Zakharov and K. P. Bryliakov, *ACS Catal.*, 2017, **7**, 2868–2877; (d) W. Zhao, E. Yue, X. Wang, W. Yang, Y. Chen, X. Hao, X. Cao and W.-H. Sun, *J. Polym. Sci., Part A: Polym. Chem*., 2017, **55**, 988–996; (e) N. E. Mitchell, W. C. Anderson, B. K. Long, *J. Polym. Sci., Part A: Polym. Chem*., 2017, **55**, 3990–3996; (f) E. Yue, Y. Zeng, W. Zhang, Y. Sun, X.-P. Cao and W.-H. Sun, *Sci. China Chem*., 2016, **59**, 1291–1300; (g) W. Zhang, S. Wang, S. Du, C.-Y. Guo, X. Hao and W.-H. Sun, *Macromol. Chem. Phys.* 2014, **215**, 1797–1809; (h) S. Wang, B. Li, T. Liang, C. Redshaw, Y. Li and W.-H. Sun, *Dalton Trans.*, 2013, **42**, 9188–9197; (i) T. M. Smit, A. K. Tomov, G. J. P. Britovsek, V. C. Gibson, A. J. P. White and D. J. Williams, *Catal. Sci. Technol*., 2012, **2**, 643–655; (j) W. Zhao, J. Yu, S. Song, W. Yang, H. Liu, X. Hao, C. Redshaw and W.-H. Sun, *Polymer*, 2012, **53**, 130–137; (k) X. Cao, F. He, W. Zhao, Z. Cai, X. Hao, T. Shiono, C. Redshaw and W.-H. Sun, *Polymer* 2012, **53**, 1870–1880; (l) J. Lai, W. Zhao, W. Yang, C. Redshaw, T. Liang, Y. Liu and W.-H. Sun, *Polym. Chem.*, 2012, **3**, 787 -793; (m) F. He, W. Zhao, X.-P. Cao, T. Liang, C. Redshaw and W.-H. Sun, *J. Organomet. Chem.*, 2012, **713**, 209-216; (n) J. Yu, W. Huang, L. Wang, C. Redshaw and W.-H. Sun, *Dalton Trans*., 2011, **40**, 10209–10214 (o) J. Yu, H. Liu, W. Zhang, X. Hao and W.-H. Sun, *Chem Comm*., 2011, **47**, 3257–3259; (p) L. Guo, H. Gao, L. Zhang, F. Zhu and Q. Wu, *Organometallics*, 2010, **29**, 2118–2125; (q) F. Kaul, K. Puchta, G. Frey, E. Herdtweck and W. Herrmann, *Organometallics*, 2007, **26**, 988–999; (r) G. J. P. Britovsek, V. C. Gibson, O. D. Hoarau, S. K. Spitzmesser, A. J. P. White and D. J. Williams, *Inorg. Chem*., 2003, **42**, 3454–3465.
5. (a) L. Wang, W.-H. Sun, L. Han, H. Yang, Y. Hu and X. Jin, *J. Organomet. Chem*., 2002, **658**, 62–70; (b) W.-H. Sun, S. Jie, S. Zhang, W. Zhang, Y. Song and H. Ma, *Organometallics*, 2006, **25**, 666–677; (c) J. D. A. Pelletier, Y. D. M. Champouret, J. Cardaso, L. Clowes, M. Gañete, K. Singh, V. Thanarajasingham and G. A. Solan, *J. Organomet. Chem*., 2006, **691**, 4114–4123; (d) S. Jie, S. Zhang, K. Wedeking, W. Zhang, H. Ma, X. Lu, Y. Deng and W.-H. Sun, *C. R. Chim*., 2006, **9**, 1500–1509; (e) S. Jie, S. Zhang, W.-H. Sun, X. Kuang, T. Liu and J. Guo, *J. Mol. Catal. A: Chem*., 2007, **269**, 85–96; (f) S. Jie, S. Zhang and W.-H. Sun, *Eur. J. Inorg. Chem*., 2007, **35**, 5584–5598; (g) M. Zhang, P. Hao, W. Zuo, S. Jie and W.-H. Sun, *J. Organomet. Chem.,* 2008, **693**, 483–491; (h) M. Zhang, R. Gao, X. Hao and W.-H. Sun, *J. Organomet. Chem*., 2008, **693**, 3867–3877.
6. (a) L. Xiao, R. Gao, M. Zhang, Y. Li, X. Cao and W.-H. Sun, *Organometallics*, 2009, **28**, 2225–2233; (b) R. Gao, Y. Li, F. Wang, W.-H. Sun and M. Bochmann, *Eur. J. Inorg. Chem.*, 2009, 4149–4156; (c) Y. Chen, P. Hao, W. Zuo, K. Gao and W.-H. Sun, *J. Organomet. Chem.,* 2008, **693**, 1829–1840; (d) W.-H. Sun, P. Hao, S. Zhang, Q. Shi, W. Zuo, X. Tang and X. Lu, *Organometallics*, 2007, **26**, 2720–2734
7. K. Wang, K. Wedeking, W. Zuo, D. Zhang and W.-H. Sun, *J. Organomet. Chem*., 2008, **693**, 1073–1080.
8. S. Zhang, W.-H. Sun, T. Xiao and X. Hao, *Organometallics*, 2010, **29**, 1168–1173.
9. (a) W. Zhang, W. Chai, W.-H. Sun, X. Hu, C. Redshaw and X. Hao, *Organometallics*, 2012, **31**, 5039–5048; (b) W.-H. Sun, S. Kong, W. Chai, T. Shiono, C. Redshaw, X. Hu, C. Guo and X. Hao, *Appl. Catal., A*., 2012, **447–448**, 67–73.
10. (a) J. Ba, S. Du, E. Yue, X. Hu, Z. Flisak and W.-H. Sun, *RSC Adv*., 2015, **5**, 32720–32729; (b) Y. Zhang, C. Huang, X. Hao, X. Hu and W.-H. Sun, *RSC Adv*., 2016, **6**, 91401–91408.
11. (a) F. Huang, W. Zhang, E. Yue, T. Liang, X. Hu and W.-H. Sun, *Dalton Trans*., 2016, **45**, 657–666; (b) F. Huang, W. Zhang, Y. Sun, X. Hu, G. A. Solan and W.-H. Sun, *New J. Chem.*, 2016, **40**, 8012–8023; (c) F. Huang, Q. Xing, T. Liang, Z. Flisak, B. Ye, X. Hu, W. Yang and W.-H. Sun, *Dalton Trans*., 2014, **43**, 16818–16829; (d) Y. Zhang, H. Suo, F. Huang, T. Liang, X. Hu and W.-H. Sun, *J. Polym. Sci. Part A. Polym. Chem*., 2017, **55**, 830–842.
12. V. K. Appukuttan, Y. Liu, B. C. Son, C. -S. Ha, H. Suh and I. Kim, *Organometallics*, 2011, **30**, 2285–2294.
13. (a) S. Du, W. Zhang, E. Yue, F. Huang, T. Liang and W.-H. Sun, *Eur. J. Inorg. Chem*., 2016, 1748–1755; (b) S. Du, X. Wang, W. Zhang, Z. Flisak, Y. Sun and W.-H. Sun, *Polym. Chem*., 2016, **7**, 4188–4197; (c) C. Huang, S. Du, G. A. Solan, Y. Sun and W.-H. Sun, *Dalton Trans.*, 2017, **46**, 6948–6957; (d) H. Suo, I. I. Oleynik, C. Bariashir, I. V. Oleynik, Z. Wang, G. A. Solan, Y. Ma, T. Liang and W.-H. Sun, *Polymer*, 2018, **149**, 45-54; (e) C.Bariashir, Z.Wang, H. Suo, Z. Muhammad, G. A. Solan, Y. Ma, T. Liang and W.-H. Sun, *Eur. Polym. J*., 2019, **110**, 240-251.
14. Z, Wang, G. A, Solan, Q. Mahmood, Q. Liu, X. Hao, and W.-H. Sun, *Organometallics*, 2018, **37**, 380–389.
15. (a) B. Pan, B. Liu, E. Yue, Q. Liu, X. Yang, Z. Wang and W.-H. Sun, *ACS Catal*., 2016, **6**, 1247-1253; (b) Z. Wang, X. Chen, B. Liu, Q. Liu, G. A. Solan, X. Yang and W.-H. Sun, *Catal. Sci. Technol*., 2017, **7**, 1297-1304; (c) Z. Wang, B. Pan, Q. Liu, E. Yue, G. A. Solan, Y. Ma and W.-H. Sun, *Catal. Sci. Technol*., 2017, **7**, 1654-1661; (d) Z. Wang, Y. Li, Q.-b. Liu, G. A. Solan, Y. Ma and W.-H. Sun, *ChemCatChem*, 2017, **9**, 4275 – 4281.
16. (a) F. W. Vierhapper and E. L. Eliel, *J. Org. Chem*., 1975, **19**, 2729-2734; (b) T. W. Bell, A. B. Khasanov, and M. G. B. Drew, *J. Am. Chem. Soc*. 2002, **124**, 14092–14103.
17. R. P. Thummel and Y. Jahng, *J. Org. Chem*., 1985, **50**, 2407–2412.
18. C. Bariashir, Z. Wang, S. Du, G. A. Solan, C. Huang, T. Liang and W.-H. Sun, *J. Polym. Sci., Part A: Polym. Chem*., 2017, **55**, 3980–3989.
19. G. J. P. Britovsek, S. A. Cohen, V. C. Gibson and M. V. Meurs, *J. Am. Chem. Soc*., 2004, **126**, 10701–10712.
20. D. J. Jones, V. C. Gibson, S. M. Green, P. J. Maddox, A. J. P. White and D. J. Williams, *J. Am. Chem. Soc*. 2005, **127**, 11037–11046; (b) A. K. Tomov, V. C. Gibson, G. J. P. Britovsek, R. J. Long, M. van Meurs, D. J. Jones, K. P. Tellmann and J. J. Chirinos, *Organometallics*, 2009, **28**, 7033 – 7040.
21. T. Xiao, P. Hao, G. Kehr, X. Hao, G. Erker and W.-H. Sun, *Organometallics*, 2011, **30**, 4847 – 4853.

22. (a) A. S. Abu-Surrah, K. Lappalainen, U. Piironen, P. Lehmus, T. Repo and M. Leskela, *J. Organomet. Chem*., 2002, **648**, 55–61; (b) W.-H. Sun, X. Tang, T. Gao, B. Wu, W. Zhang and H. Ma, *Organometallics*, 2004, **23**, 5037–5047.
23. (a) N. V. Semikolenova, V. A. Zakharov, E. P. Talsi, D. E. Babushkin, A. P. Sobolev, L.G. Echevskaya and M. M. Khysniyarov, *J. Molecular Catal. A: Chem*. 2002, **182–183**, 283–294; (b) E. Talsi and K. Bryliakov, Chapter 4, *CRC Press*. Taylor & Francis Group, 2017.
24. (a) G. M. Sheldrick, *Acta Cryst*. 2015, **A71**, 3–8. (b) G. M. Sheldrick, *Acta Crystallogr., Sect. C: Struct. Chem*. 2015, **C71**, 3–8

Journal Name

ARTICLE

GRAPHICAL ABSTRACT

Bis(imino)pyridines fused with 6- and 7-membered carbocylic rings as *N,N,N*-scaffolds for cobalt ethylene polymerization catalysts

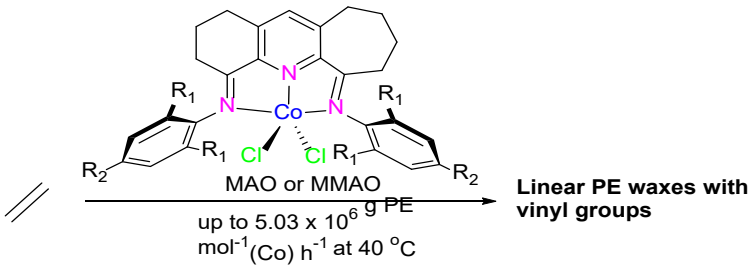

The mixed carbocyclic-fused bis(arylimino)pyridine-cobalt(II) chlorides, on activation with either MAO or MMAO, displayed high activities for ethylene polymerization affording linear polyethylene waxes; high selectivity for vinyl end-groups are a feature of the MAO-promoted systems.